DESIGN AND IMPLEMENTATION OF A LAND SURFACE PROCESSES PARAMETERIZATION IN A MESO-BETA SCALE MODEL

P. BOUGEAULT, B. BRET, P. LACARRERE, and J. NOILHAN
CNRM - TOULOUSE, France

1 - INTRODUCTION

Natural land surfaces are not homogeneous over the resolvable scales of atmospheric models. Therefore, these models must account for the subgrid-scale variability of underlying surfaces to determine the grid averaged surface energy budget. The most difficult problem concerns the partition of available energy into sensible and latent heat fluxes, hence the modeling of regional evapotranspiration, since the moisture availability, defined in a broad sense (see Bougeault, 1988 for a review on this parameter), will generally depend on numerous factors : the soil type, the soil moisture content, the type, age and density of vegetation. Each of these factors has its own subgrid-scale variability. If we assume we can compute local evapotranspiration, when we know local values of the controlling factors, we are still confronted by the necessity of averaging this result over a model grid-box, taking into account the statistical properties of the existing distribution of the controlling factors inside the grid-box. Generally, this will require the knowledge of mean values, variances but also possible correlations of these elements inside this grid-box. The response of a parameterization scheme to this averaging process is expected to be quite non-linear, because of the wide range of observed variation of evapotranspiration, and of the non-linear dependance of local evapotranspiration on the controlling parameters. However, the exact nature and severity of this non-linearity is, at the present time, not known.

The present paper is based on a quite optimistic point of view. In the authors' opinion, simple, empirical methods should first be evaluated against existing observations, before going on to more complicated ones. The development of this "optimistic" approach is as follows. First of all, it is based on the calibration of a parameterization scheme against local measurements, which allows for the determination of the most sensitive parameters. These parameters will clearly require the greatest attention, when trying to obtain area-averaged values. Secondly, it relies on the progressive elaboration of maps of parameters, by various methods, that will be required anyway if more sophisticated approaches are necessary in the future. Thus, the present work must be viewed as a first,empirical attempt to implement a simple grid-averaging method. Its prime merit is that it can be done with the existing information, and that it will set a lower limit for the performances of an averaging method.

The paper will proceed as follows : we present the basic parameterization scheme in Section 2, along with a list of parameters that need specification to be applied in a mesoscale model (Table 1). These parameters have been deliberately kept to a minimum number, in order to simplify the further work of gathering information, under the form of maps.In Section 3, we discuss one-dimensional calibration runs. These runs,using the field measurements of the Hapex-Mobilhy experiment (André

Table 1.

	notations
Primary parameters	
Dominant type of vegetation	
Dominant type of soil texture	
Secondary parameters	
Saturated volumetric moisture content	w_{sat}
Wilting point volumetric water content	w_{wilt}
Slope of the retention curve	b
Soil thermal coefficient at saturation	C_{gsat}
Value of C_1 at saturation	C_{1sat}
Value of C_2 for $w_2=0.5w_{sat}$	C_{2ref}
Coefficients of w_{geq} formulation	a,p
Depth of the soil column	d_2
Fraction of vegetation	veg
Minimum surface resistance	R_{smin}
Leaf Area Index	LAI
Roughness length	z_o
Albedo	α
Emissivity	ϵ

#	Site	Vegetation	Texture	ω_g	ω_2	z_o (m)	α	LAI	R_{SMIN} (s/m)	VEG
1	Estampon	Coniferous	Sand	0.14	0.20	1.00	0.10	2.3	100	0.99
2	Caumont	Crop / sojà	Loam	0.26	0.26	0.02	0.24	1.0	40	0.70
3	Castelnau	Crop / maize	Loam	0.18	0.25	0.02	0.25	0.3	40	0.40
4	Lubbon 2	Crop / maize	Sand	0.17	0.17	0.10	0.15	2.0	40	0.80
5	Tieste	Crop / maize	Loam	0.20	0.26	0.05	0.23	0.5	40	0.40
6	Fusterou.	Crop / maize	Loam	0.16	0.27	0.06	0.25	1.0	40	0.50
7	Lubbon 1	Crop / oats	Sand	0.17	0.17	0.10	0.20	3.0	40	0.90
8	Orchards, Vineyards...		Loam	0.18	0.25	0.15	0.18	1.0	80	0.40
9	Desert		Sand	0.06	0.12	0.10	0.20	0.1	999	0.10
10	Desert		Loam	0.08	0.15	0.10	0.20	0.1	999	0.10

TABLE 2

Dominant Surface Type (DST)	n°	VEG	LAI	Z_o (m)	R_{SMIN} (s/m)
Water	0	0	0.001	0.001	999
Desert	1	0.10	0.1	0.15	999
Orchards, vineyards...	2	0.40	1.0	0.15	80
Mediterranean vegetation	3	0.40	1.0	0.15	80
Crops	4	0.50	1.0	0.15	40
Grasslands	5	0.60	1.5	0.15	40
Coniferous forests	6	0.99	3.0	1.0	100
Deciduous forests	7	0.90	3.0	1.0	100

TABLE 3

et al., 1988), which have been done in large number, allow for the determination of optimal values of those parameters which are not well known, for the scheme to be able to reproduce local measurements of the fluxes of sensible and latent heat, into the atmosphere, and of the heat flux into the ground. The general result of these experiments is summarized in Table 2, whereby the list of optimal values of all the parameters of the scheme is given for any situation that has been experimentally documented during the Hapex-Mobilhy field experiment. Section 4 deals with the way of deriving maps of these parameters, based on various information sources. The 3D numerical model, using the parameterization scheme and the maps of parameters previously described is then used to simulate one day of the Hapex-Mobilhy experiment : June 16, 1986. The results of this simulation are described in Sections 5 and 6, and compared to available observations.
Note than an expanded version of the present paper can be found in Bougeault et al. (1988).

2 - FORMULATION OF THE BASIC PARAMETERIZATION SCHEME

We use for the present study the parameterization scheme proposed by Noilhan and Planton (1989, hereafter referred to as NP89). This scheme allows for the computation of the different components of the surface energy and moisture budgets over various types of soil and vegetation, and for the interception of rain or dew on the vegetation.

The scheme has five prognostic variables, which are the surface temperature T_g, the deep soil temperature T_2, the amount of moisture retained at the surface of the vegetation W_r, the superficial soil volumetric water content W_g, finally the vertically integrated soil volumetric water content W_2. The prognostic equations for these variables are as follow :

$$\frac{\partial T_s}{\partial t} = C_T G - 2\pi (T_s - T_2) / \tau , \qquad (1)$$

$$\frac{\partial T_2}{\partial t} = (T_s - T_2) / \tau , \qquad (2)$$

$$\frac{\partial W_r}{\partial t} = veg\ P - (E_v - E_{tr}) - R_r , \quad 0 \leq W_r \leq W_{rmax} , \qquad (3)$$

$$\frac{\partial W_g}{\partial t} = C_1 (P_g - E_g)/\rho_w d_1 - C_2 (w_g - w_{geq}) , \quad 0 \leq W_g \leq W_{sat} , \qquad (4)$$

$$\frac{\partial W_2}{\partial t} = (P_g - E_g - E_{tr})/\rho_w d_2 , \quad 0 \leq W_2 \leq W_{sat} . \qquad (5)$$

The definition of the various parameters found in (1) - (5) is as follows. The most important one, "veg" is the "fraction of vegetation" within the grid. It must be understood as a foliage shielding factor of the ground from solar radiation. A fraction (1-veg) of incoming solar radiation will effectively reach the ground. Also, a fraction (1-veg) of the rainfall or dew will directly reach the ground.

τ is the diurnal time constant (τ = 86 400 s). C_T is the thermal inertia of the soil-vegetation medium. It is expressed as :

$$C_T = ((1-veg)/C_G + veg/C_v)^{-1} \quad (6)$$

where $C_v = 10^{-3} Km^2 J^{-1}$ is an arbitrarily large value which means that the vegetation has a very weak thermal inertia, and C_G, the thermal inertia of the ground, is parameterized as :

$$C_G = C_{Gsat} (W_{sat}/W_2)^{b/2\log 10} . \quad (7)$$

G is equal to the sum of three components :

$$G = R_n - H - LE \quad (8)$$

where R_n is the net radiation, H and LE the sensible and latent heat fluxes respectively.

The net radiation R_n at the surface is the sum of the absorbed fractions of the incoming solar radiation R_G, and of the atmospheric infrared radiation R_A, reduced by the emitted infrared radiation.

$$R_n = R_G(1 - \alpha) + \epsilon (R_A - \sigma T_s^4), \quad (9)$$

where the albedo α and the emissivity ϵ combine the soil and the vegetation reflectivities. σ is the Stefan-Boltzmann constant. The turbulent fluxes towards the atmosphere are computed by the classical aerodynamic formulae. For the sensible heat flux

$$H = \rho_a C_p C_H V_a (T_s - T_a) \quad (10)$$

where C_p is the specific heat, ρ_a, V_a and T_a the air density, wind speed and temperature at the atmospheric level Z_a, and C_H the drag coefficient for heat, depending on the stability of the surface layer.

The water vapor flux E is split into evaporation from the soil surface E_g, transpiration from the vegetation E_{tr} and direct evaporation from the water retained at the surface of the vegetation E_v-E_{tr}. Hence, the total evapotranspiration is E_v. These various components are parameterized according to

$$E_g = (1-veg) \rho_a C_H V_a (h_u q_{sat}(T_s) - q_a), \quad (11)$$

$$E_v = veg \rho_a C_H V_a h_v (q_{sat}(T_s) - q_a) \quad (12)$$

where q_a is the atmospheric specific humidity at level Z_a, h_u is the relative humidity of the superficial ground

$$\begin{aligned} h_u &= (1 - \cos(W_g \pi / W_{f1}))/2 \quad \text{if } W_g < W_{f1} \\ &= 1 \quad \text{if } W_g > W_{f1} \end{aligned} \quad (13)$$

with $w_{f1} = 0.75\ w_{sat}$ the field capacity.

The Halstead coefficient h_v takes into account the direct evaporation from the fraction δ of the foliage surface covered by water, and the transpiration from the fraction $(1-\delta)$:

$$h_v = (1-\delta) R_a/(R_a+R_s) + \delta \quad (14)$$

with $\delta = (W_r/W_{rmax})^{2/3}$, $R_a = (C_H V_a)^{-1}$ the atmospheric resistance, and R_s

the surface resistance. The expression of R_s, derived from Jarvis (1976), incorporates the various influences of the leaf area index LAI, the solar radiation, the atmospheric water vapor deficit, the air temperature, and the soil moisture content under the empirical form

$$R_s = R_{smin} (LAI)^{-1} F_1 F_2^{-1} F_3^{-1} F_4^{-4} \quad (15)$$

R_{smin} is the minimum stomatal resistance of a single leaf, which is supposed to be species-dependent, and also may vary according to the degree of maturity for a given crop. The exact formulation of F_1, F_2, F_3, F_4, can be found in NP89 and is not relevant in the present paper.

In (3) P is the total precipitation rate reaching the surface before interception by the vegetation and P_r is the runoff of the interception reservoir. This runoff occurs when W_r exceeds W_{rmax}, which depends on the density of the canopy according to an empirical formula :

$$W_{rmax} = 0.2 \text{ veg LAI (mm)} \quad (16)$$

In (4), P_g is the flux of liquid water reaching the surface after interception. E_g the evaporation from the soil surface and w_{geq} an equilibrium value of the superficial moisture content which has been parameterized as a function of w_2 and of the type of soil. d_1 is an arbitrary normalization depth of 10 cm. C_1 and C_2 are two coefficients which depend on the type of soil and on the soil moisture content (see NP89 for the formulation).

Finally in (5) d_2 is the total depth of soil active in the water budget.

The parameters that need to be specified in order to implement the NP89 scheme on a local basis are summarized in Table 1. Among these, the ones which describe the thermal and hydraulic properties of the ground itself can be assigned a reasonable value from the knowledge of the soil texture alone, thanks to former work by Cosby et al. (1984), and by the calibrations presented by NP89. This is the case for w_{sat} , w_{wilt}, b, C_{Gsat}, C_{1sat}, C_{2ref}, a and p. The depth of the active soil column d_2, on the other hand, needs an independant specification. The remaining parameters either concern the type and density of the vegetation (veg, R_{smin}, LAI) or are global concepts which incorporate information from several sources (Z_o, α , ε).Those parameters are the most difficult to determine for the use in a 3D model. The strategy we have developed consists in obtaining representative values of these parameters for each type of vegetation cover that has been sampled during the field experiment. This is done by a series of trial-and-error one-dimensional experiments. Then, these optimal values are empirically combined to obtain values representative of the grid-box.

3 - ONE-DIMENSIONAL CALIBRATION EXPERIMENTS OF THE SCHEME

The main originality of the calibration experiments in this program was to use a 1D version of the physical package of the mesoscale model which was to be later used for the integration itself. This mean that the surface scheme was run interactively with the remaining of the model physics (boundary layer and radiation subschemes) for 24 hour periods starting and finishing at midnight. In particular, the atmospheric parameters v_a, q_a, T_a at level Z_a were not imposed, but predicted by the model. As the atmosphere is not 1D, it was necessary to implement a method to constrain the 1D model to follow that part of the evolution

which is not related to the surface processes. Therefore, the geostrophic wind, as well as the horizontal and vertical advection terms were deduced from mesoscale analyses (Mercusot et al., 1986) to force the 1D model. In all cases, the model was initialized with the observed sounding at midnight and with the soil moisture content derived from the neutron probe observations. The soil parameters were set to the value derived from Clapp and Hornberger (1978), in agreement with the results of the textural analysis at each site.

All parameters that could be infered from observations have been specified in this way. This was the case for the albedo, the LAI,which were known for each site. The roughness length has been taken equal to one tenth of the vegetation height. The minimumm surface resistance R_{smin} has been deduced following Monteith (1976), and the emissivity was given the constant value of 0.95. Finally, in most cases, only the fraction of vegetation veg was left unknown. This parameter was adjusted so as to reproduce as accurately as possible the soil heat flux.

The quality of the ensemble of parameters was checked by comparing the 24 h predicted fluxes of latent and sensible heat with the observations of the Samer and Hydra stations (André et al., 1988).

The present paper will show only one example of such comparison. This is the case number 3 discussed in NP88. It illustrates an example with a significant fraction of bare ground (veg = 0.4). The measurements are taken in Castelnau in a field of corn (0.2 m high) over a loamy soil. The initial values of the soil moisture are : W_g = 0.18, W_2 = 0.25, and the other parameters are set as Z_o = 2 cm, α = 0.25, LAI = 0.3, R_{smin} = 40 s/m. The results are shown in Fig. 1. We observe high values of G, reaching some 100 W/m² at noon, since the amount of solar radiation reaching the ground is important. The model predicts the observed daily variations of G reasonably well. The magnitudes and diurnal variations of LE and H are also correctly simulated.

As a general result of the 1D calibration/test runs, we have been able to assemble a general table of the optimal parameters for every situation which had been experimentally documented. This is reproduced in Table 2. Note that most values are susceptible to vary slowly with time, as the crop changes, and are representative only for a period extending to a few days before and after the test.

4 - MAPPING THE PARAMETERS FOR THE 3D MODEL

The domain of integration of the 3D atmospheric model is shown in Fig. 2. It is much wider than the 100 x 100 km² Hapex-Mobilhy study area to eliminate the influence of possible boundary reflections. The domain encompasses large portions of the Massif Central and Pyrénées mountains, parts of the Atlantic ocean and of the Mediterranean, and extends to the South as far as the high Spanish Plateau. The grid size is 10 km, and the total area extends by about 400 x 400 km².

Three main sources of information are presently available on this domain. The first one consists in several existing maps of soil types. These maps have been processed by Mascart et al. (1988) to produce a synthetic result for each grid box of the mesoscale model. First of all, the dominant textural class has been identified, according to a classification compatible with the one of Clapp and Hornberger (1978), used by the NP89 scheme. Secondly, the depth d_2 of the active soil layer

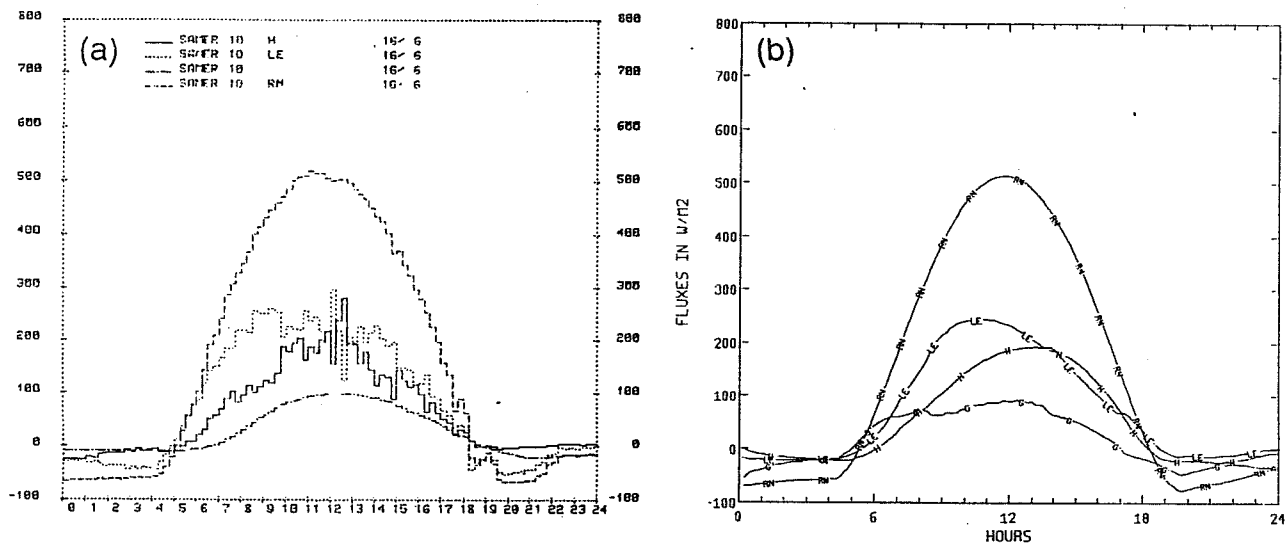

Fig. 1 : Diurnal variations of observed (a) and simulated (b) surface fluxes (in W/ m²) for Case 3 of NP88 : Net radiation R_n, latent heat flux LE, sensible heat flux H, and soil heat flux G.

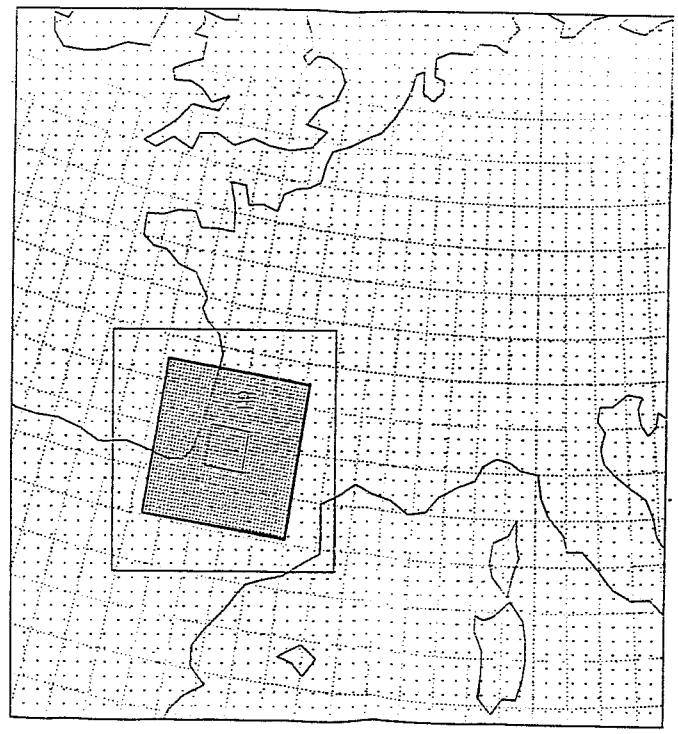

Fig. 2 : The domain of integration of the mesoscale model used in the present study.

has been mapped. Over the study area,its value is ranging from 40 to 80 cm. On the other hand, soils less than 20 cm deep are to be found in the mountainous areas and over the Spanish plateau.

The second source of information is given by the series of Meteosat satellite infrared and visible images which have been archived during the S.O.P. These images were processed by R.M. Thépenier at the CNRM, following the method of Dedieu et al. (1987) to produce maps of the mean albedo for each month of the S.O.P., on the grid of the mesoscale model. Finally, the third source of information lies in the NOAA AVHRR data series, which are available between 2 and 4 times a day during the S.O.P. These data have been processed to obtain NDVI images (Phulpin and Jullien, 1988). The ultimate goal of this research program is to derive from these NDVI maps as much information related to the type of vegetation, and the parameters veg, R_{smin} and LAI as possible. This goal, however, has not yet been reached. For the present study, we have used only a map of 7 dominant vegetation types which has been obtained by a supervised classification method applied to a couple of cloud-free images (27 June and 10 July 1986). The details of this algorithm are given by Phulpin and Jullien (1988).This map is available with the initial AVHRR pixel resolution, i.e., close to 1 km (Fig. 3). It has been further processed to obtain the dominant vegetation type (according to the same 7 classes) in each grid-box of the mesoscale model (Fig. 4). These different maps have been used together with the information given in Table 2, to compute grid-scale values of the four remaining unknown parameters :veg, R_{smin}, LAI, and Z_o.Several algorithms have been tried, and are currently tested. The most simple was to affect for each parameter the value corresponding to the dominant type of vegetation at the scale of the model grid-box. Since the NDVI-derived classification does not differentiate different types of crops,this required a further simplification of Table 2, which was made possible by the fact that most crops have the same value of R_{smin}. Thus, a set of simplified type of vegetation parameters correspondance was elaborated, as given in Table 3. This most simple approach was tested and resulted in predictions of the mesoscale model including a high degree of noise. A more refined approach was therefore worked out. Taking advantage of the fact that the map of vegetation classes was available at the AVHRR pixel definition, the set of correspondance of Table 3 was used at this definition, and representative values of the parameters for each model grid-box were computed by averaging the values corresponding to the pixels inside each grid-box. This provides maps with smoother -and hopefully,more realistic-spatial variations of the parameters. Several combinations of the two former approaches were tried, and it was found that the most important effect was on the parameter veg. Therefore, we will show in the next section results from a simulation were the pixel-averaging method has been used only for veg (the other parameters are still set to the value corresponding to the dominant type of vegetation inside the grid-box). The field of the parameter veg obtained by the explained method is shown in Fig. 5.

The last quantities requiring a mapping are the initial value of the soil moisture contents W_r, W_g and W_2. W_r has been set to zero identically for the sake of simplicity. For W_g and W_2 an empirical procedure was defined, to take into account at best the existing information. Semi-desertic areas present in the southern part of the domain (discriminated by the condition veg $<$ 0.1) were assigned the values $W_g = 0.15\ W_{sat}$, and $W_2 = 0.3\ W_{sat}$. For all the other regions, the soil moisture content was assumed to depend mainly on the soil type. Average values of W_g/W_{sat} and W_2/W_{sat}

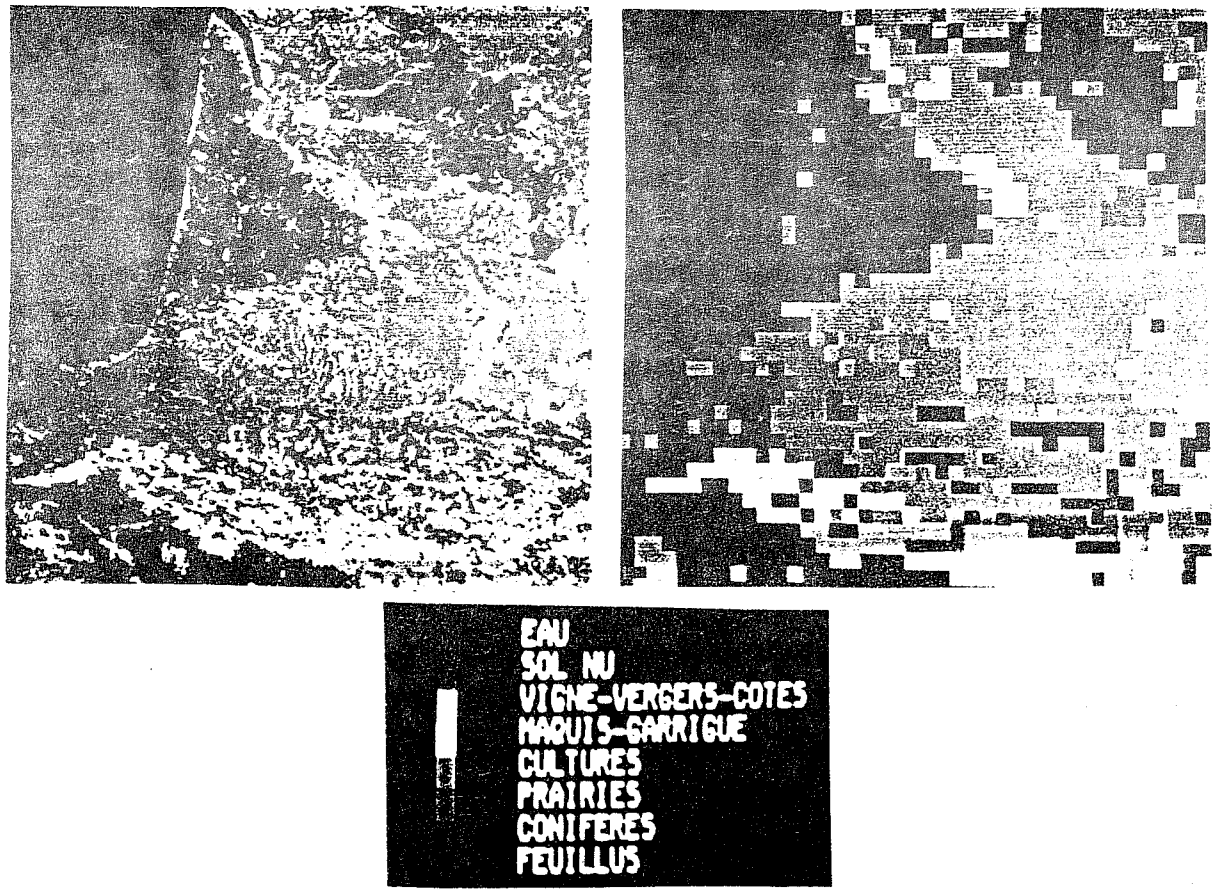

Fig. 3 : From Phulpin and Jullien (1988). A map of the vegetation type at the AVHRR pixel-scale resolution for the domain of simulation.

Fig. 4 : From Phulpin and Jullien (1988). The map of dominant vegetation type inside each grid box of the meso-scale model.

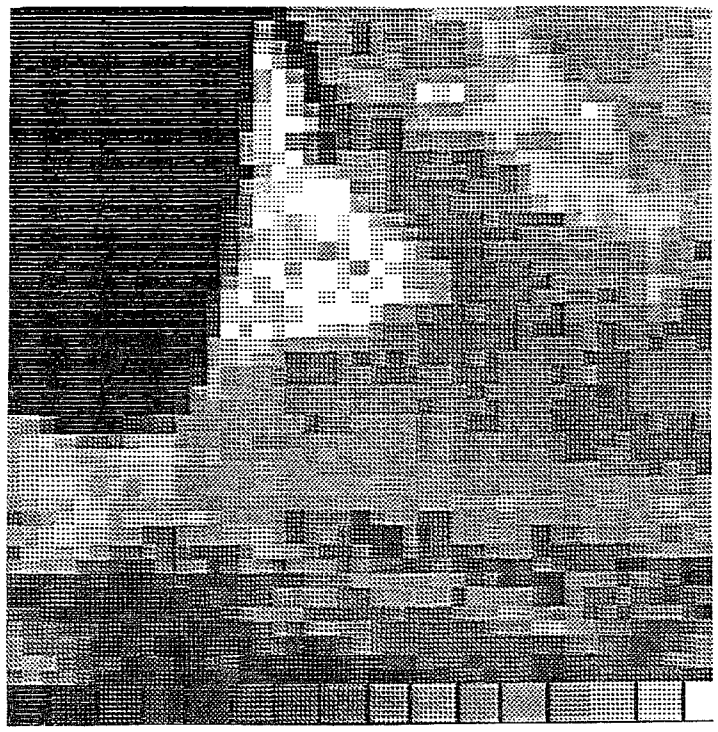

Fig. 5 : Map of the fraction of vegetation veg in each grid box of the mesoscale model, derived as explained in the text.

were estimated from the neutron soundings for each of the four textural classes which had been experimentally documented within the Hapex domain.

5 - GENERAL RESULTS OF THE JUNE 16, 1986 SIMULATION

We have chosen June 16, as a convenient day for the first test of the method, since most participants to the Hapex-Mobilhy program agreed on the fact that this day produced measurements of excellent quality. It should also be mentionned that a preliminary study (Bret and Bougeault, 1988) has shown that the atmospheric mesoscale simulation of June 16 was one of the best among the fair weather days selected for numerical experimentations. This is due to the quality of the mesoscale atmospheric analyses provided by the operational data assimilation algorithms of the French Weather Service (Durand and Bougeault, 1987).

On the area of interest, the low level flow was characterized by weak to moderate Southeastern winds during the first part of the day, associated with zero cloud cover, followed by an entry from the Atlantic Ocean of westerly maritime air, starting near 1500 Z, and reaching progressively the entire study area by 0000 Z the following day. The cloud cover was insignificant, except, on mountain areas on the border of the study area (upslope circulations) and inside the moist, maritime air, where scattered low level cumuli developed near 1500 Z, followed by more extensive cloud sheets after 1800 Z.

In order to assess the realism of the dynamic fields predicted by the model, we first compare the predicted anemometer level winds at 1200 Z and 1800 Z with observations. At 1200 Z (Fig.6), the winds are predominantly southeasterly on the study area. One note the influence of the upslope circulation towards the Pyrénées in the Southern portion of the study area, where weak, northerly winds are observed. Also, on the coast line, weak westerly flow may be interpreted as an early manifestation of the maritime entry. All these elements are correctly predicted by the model, which additionnally depicts a well organized upslope circulation over the Pyrénées. At 1800 Z (Fig. 7), westerly winds have reached the middle of the study area and there is a clear separation between the two air masses, since weak to moderate southeasterly winds persist over the eastern part of the simulation domain. The model thus correctly predicts the advance of the maritime air mass.

Similar comparisons can be made for the temperature at screen level. At 1200 Z (Fig. 8) the most striking pattern is that the Landes Forest has higher temperatures than the surrounding areas, by about 2K. This is confirmed by the observations. However, the model prediction appears to underestimate by 2-3 K the observations as much over the forest as elsewhere.

The predicted sensible and latent heat fluxes at 1200 Z, shown in Fig. 9 exhibit several interesting regional differences. Firstly, the Landes forest appears well characterized by higher values of the sensible heat flux. Forested areas have generally more than 300 W/m^2, whereas the surrounding areas have usually less. This is in agreement with the aircraft observations (see below Section 6). The forest is also visible on the latent heat flux maps, with somewhat smaller values of this flux. The second striking pattern is the very high sensible heat flux predicted over the spanish plateau in the Southwestern corner of the domain. This area is classified as semi-desertic in the vegetation map used in the model, and the specified soil moisture content is quite low. The

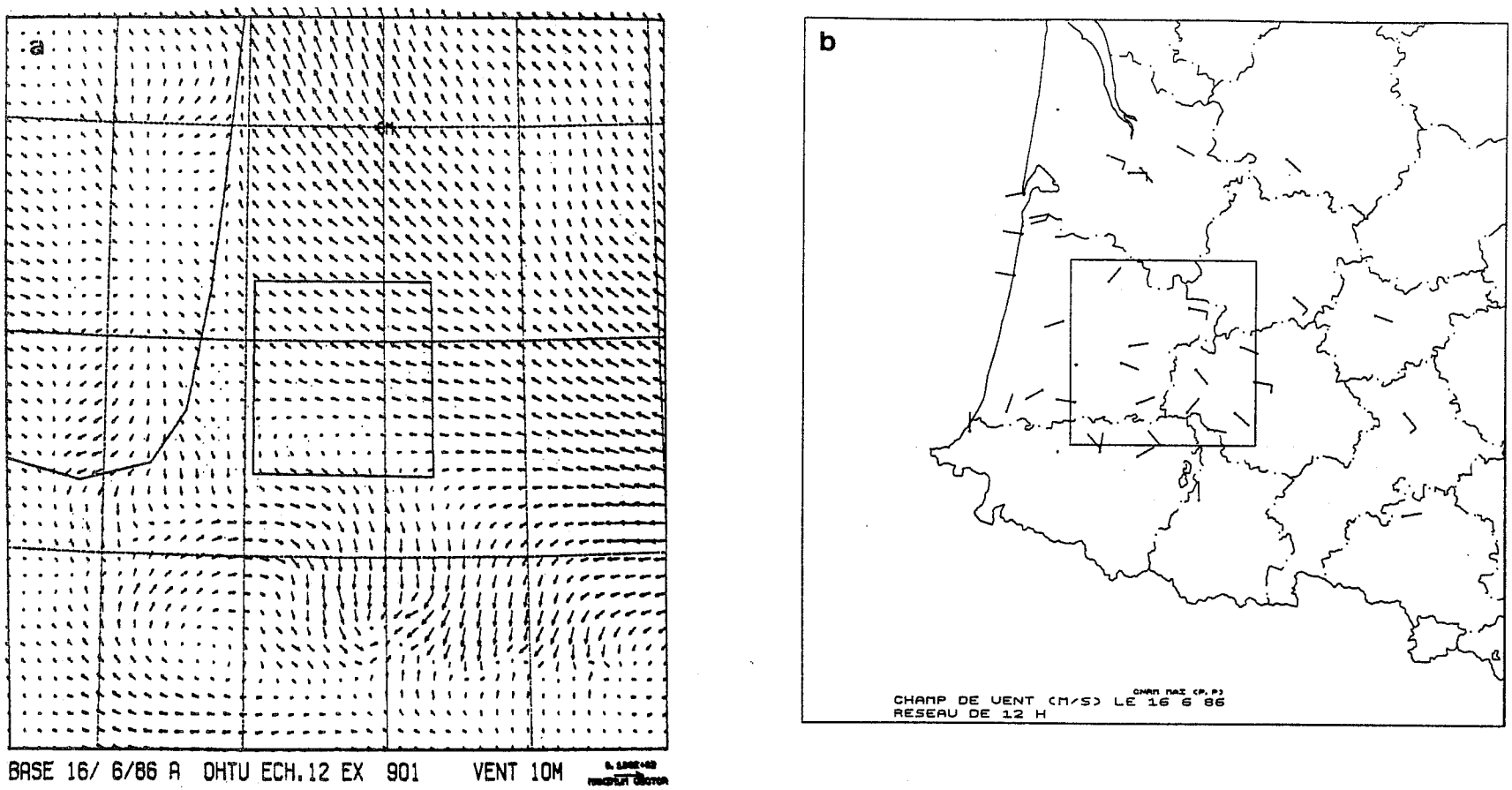

Fig. 6 : Computed (a) and observed (b) anemometer level winds at 1200 Z.

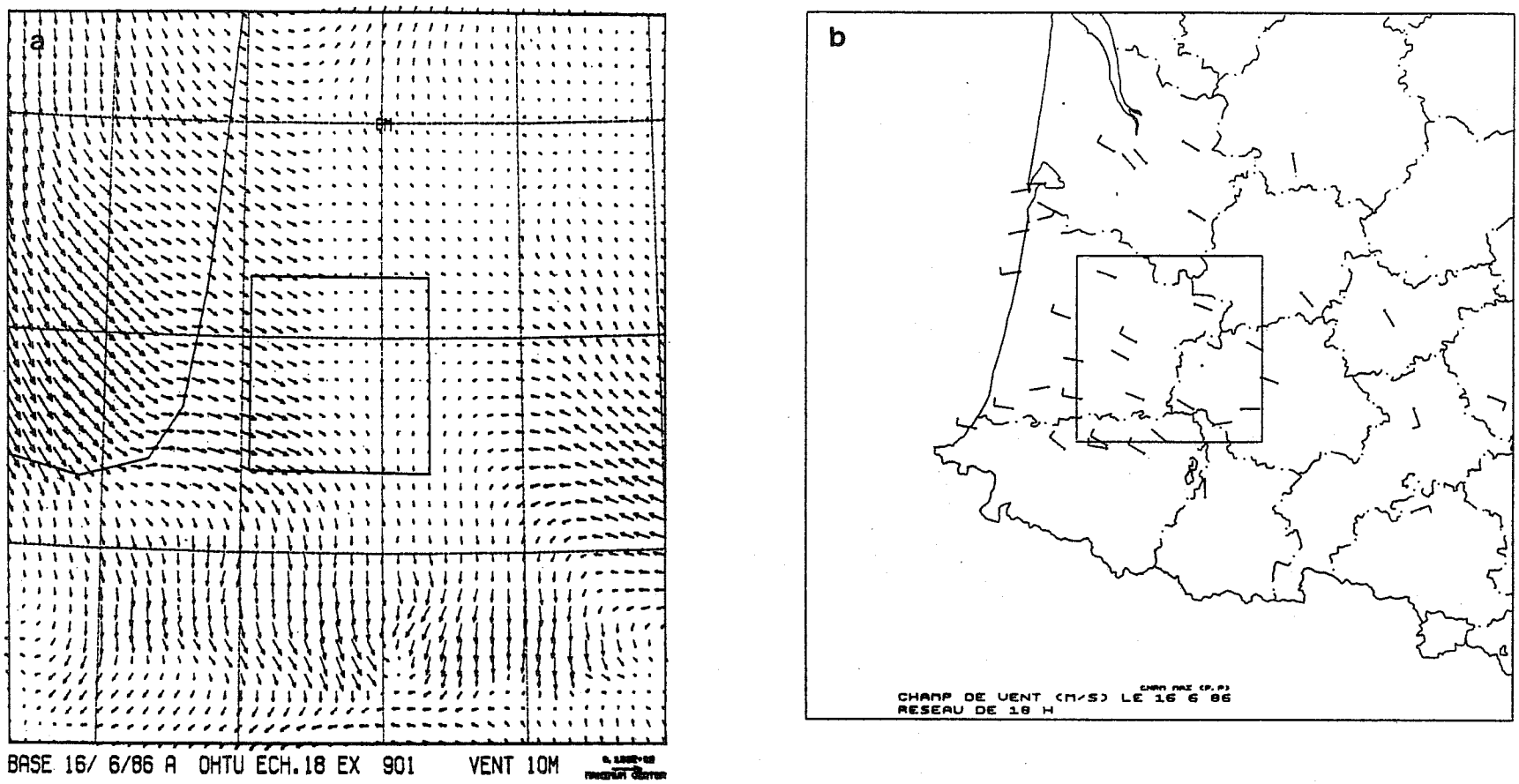

Fig. 7 : Computed (a) and observed (b) anemometer level winds at 1800 Z.

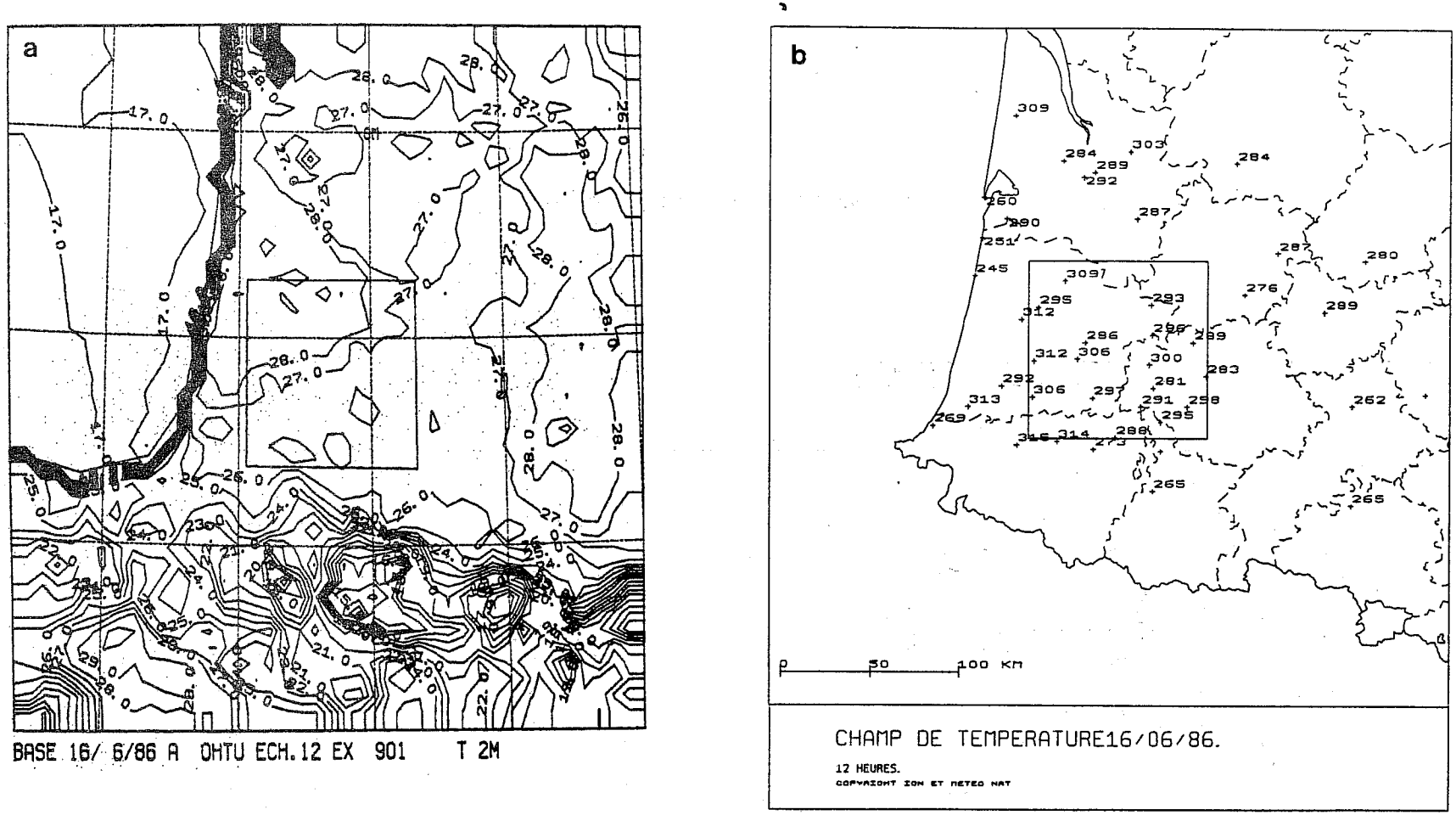

Fig. 8 : Computed (a) and observed (b) screen level temperature at 1200 Z.

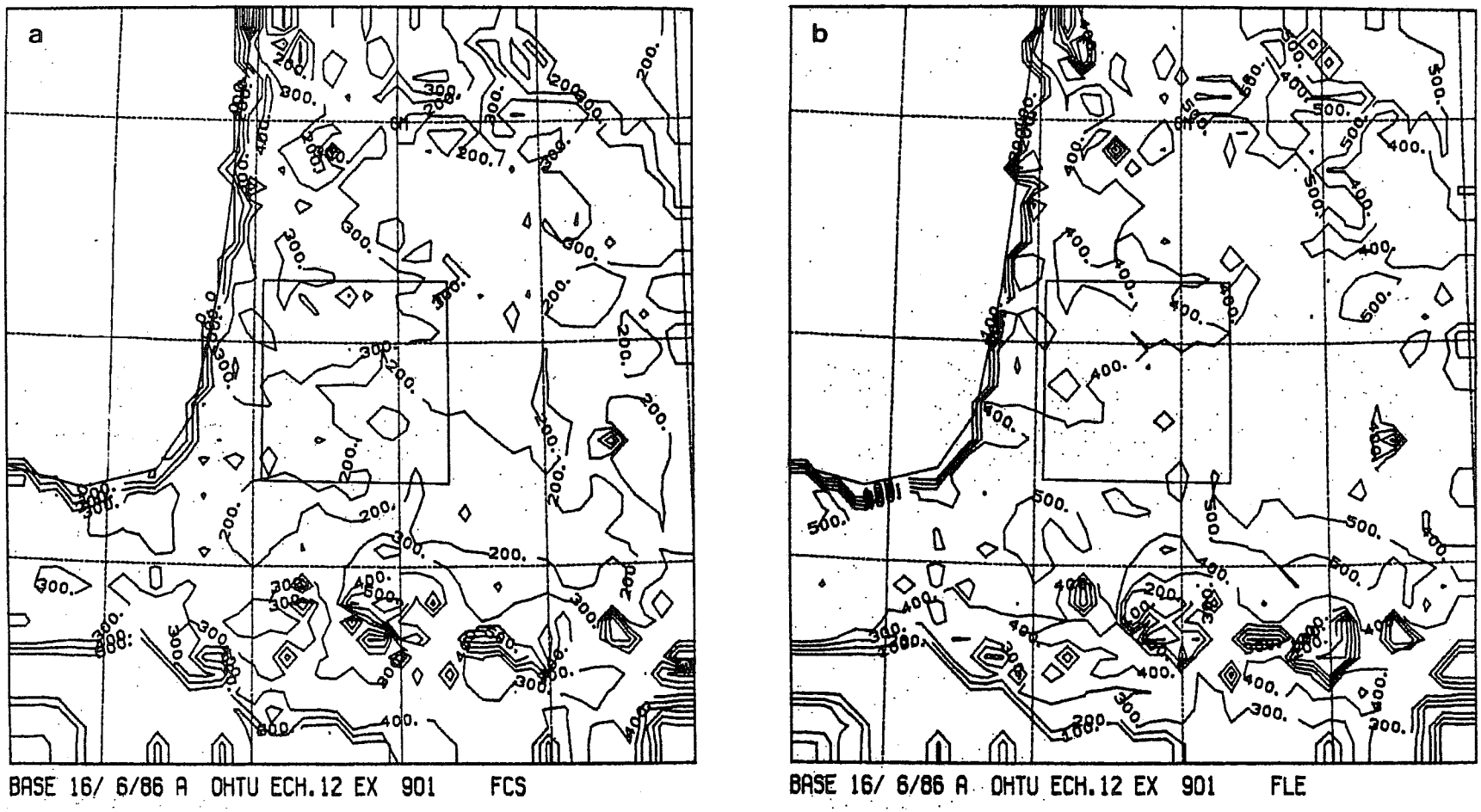

Fig. 9 : Surface sensible heat flux (a) and latent heat flux (b) predicted at 1200 Z.

superficial soil dries out during the day, leading to these very high value of the Bowen ratio. Finally, we note the relative maximum of the latent heat flux in the grasslands areas which form the northern border of the Pyrénées mountains.

Next, we will show the predicted surface temperatures at 1500 Z (Fig. 10). This time is chosen because it allows for direct comparison with the infrared satellite picture shown in Fig. 11. There is an excellent correspondance between the prediction and the observation if we ignore the very cold spots of the satellite image. They correspond to low level clouds, which have not been filtered out. It is of special interest to note that the Landes forest has colder surface temperatures than the surrounding areas where crops prevail, both in the observations and in the model prediction. This is due to the higher value of the roughness height over the forest. We have noted above that the forest is characterized by higher screen level temperatures than the surrounding areas. Here, the pattern is reversed. This is explained by a totally different value of the vertical gradient of temperature in the surface layer. The mixed crop areas, with low roughness height (Z_o = 10 cm) need to reach higher surface temperatures than the forest in order to transfer a comparable amount of heat towards the atmosphere. Maximum values of surface temperatures are noted in the mixed crop area of Gers in the southern part of the study area, as well as in the urban areas of Bordeaux and Toulouse (as well visible isolated spots on Fig. 10), and in the Spanish semi-desertic areas. All these elements are well supported by the satellite picture. Similar comparison is possible for the 0300 Z surface temperature, where the Landes forest again appears colder than the surrounding areas.

6 - DETAILED COMPARISONS WITH AVAILABLE OBSERVATIONS (SAMER, HYDRA and KING AIR)

In this section, we will go further into the comparison between existing observations and model-predicted parameters. We will first attempt a direct comparison between the diurnal cycles of temperature, wind, humidity and sensible and latent heat fluxes at specific locations and the corresponding model-predicted quantities. This is done for three specific locations : one over the forest, in the northern part of the study area, with the Hydra station ; one in the southeastern part of the study area, where four Samer stations located nearby provide a good estimate of the evaporation over crops ;the last one is in the southwestern part of the study area, to illustrate the effect of non representativeness of a Samer station. The location of the reference measurements and of the model grid points which are used for comparison is shown in Fig. 12.

The comparison of observed and predicted values of the screen level temperature and specific humidity over the forest is shown on Fig. 13 . The diurnal cycle of both quantities is correctly predicted, with an amplitude of about 15 K for the temperature, and 2 g/kg for the specific humidity. One possible discrepancy is the surface temperature at 0300 Z, where the model reaches the very low value of 10 °C. There is no reference measurement for this quantity. However, this drop seems to be overestimated, and may be due either to a too low value of the drag coefficient for heat under strong static stability conditions or to a too low value of the surface thermal inertia assumed in the model in conditions of high vegetation cover. Work is in progress to improve this aspect of the simulation.Another discrepancy with observations is the

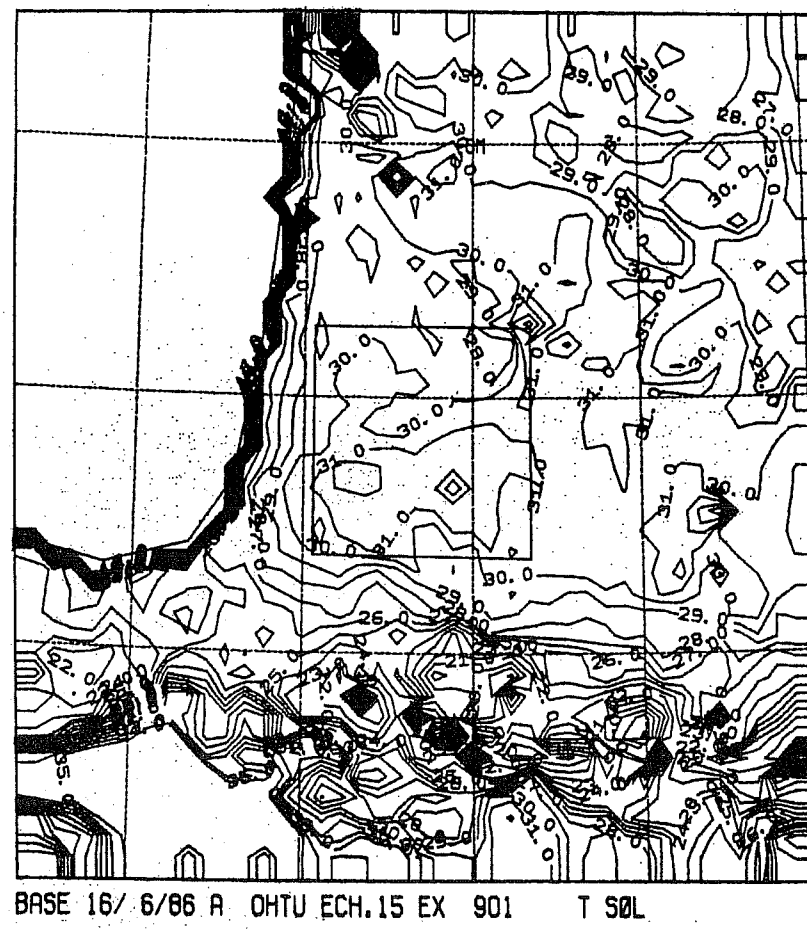

Fig. 10 : The surface temperature (T_s) predicted at 1500 Z.

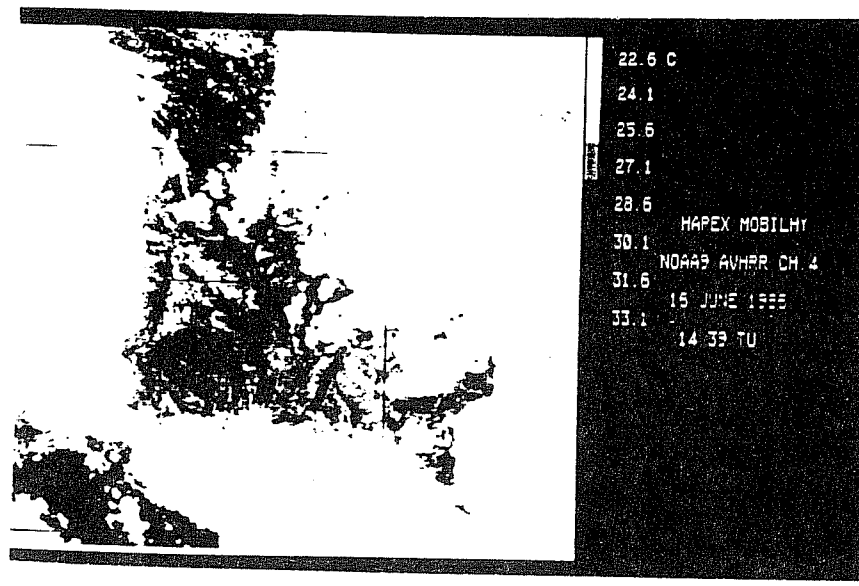

Fig. 11 : NOAA6 AVHRR Chanel 4 picture (infrared) for June 16, 1439 Z.

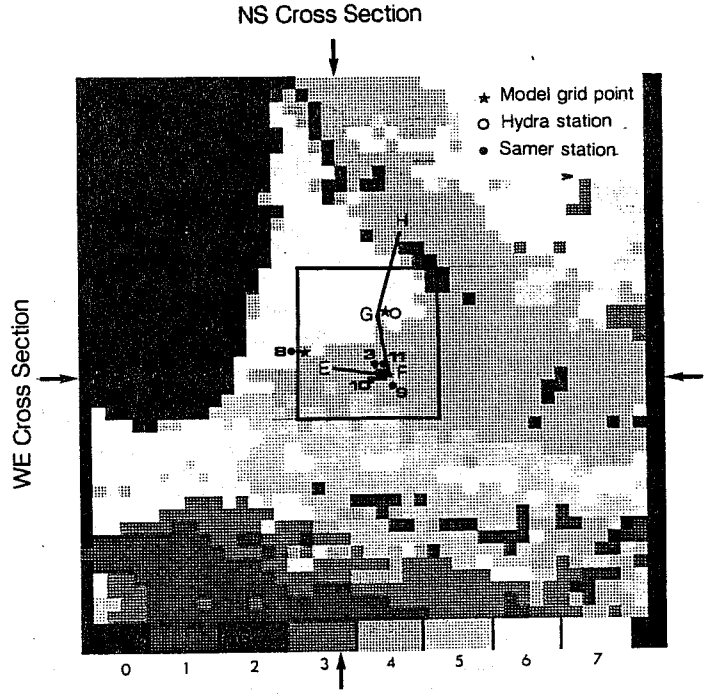

Fig. 12 : A map for the localisation of the model/observations comparison. (*) : Model grid points discussed in Section 6. Number stand for Samer stations. o: Hydra station. EFGH : King Air aircraft trajectory.

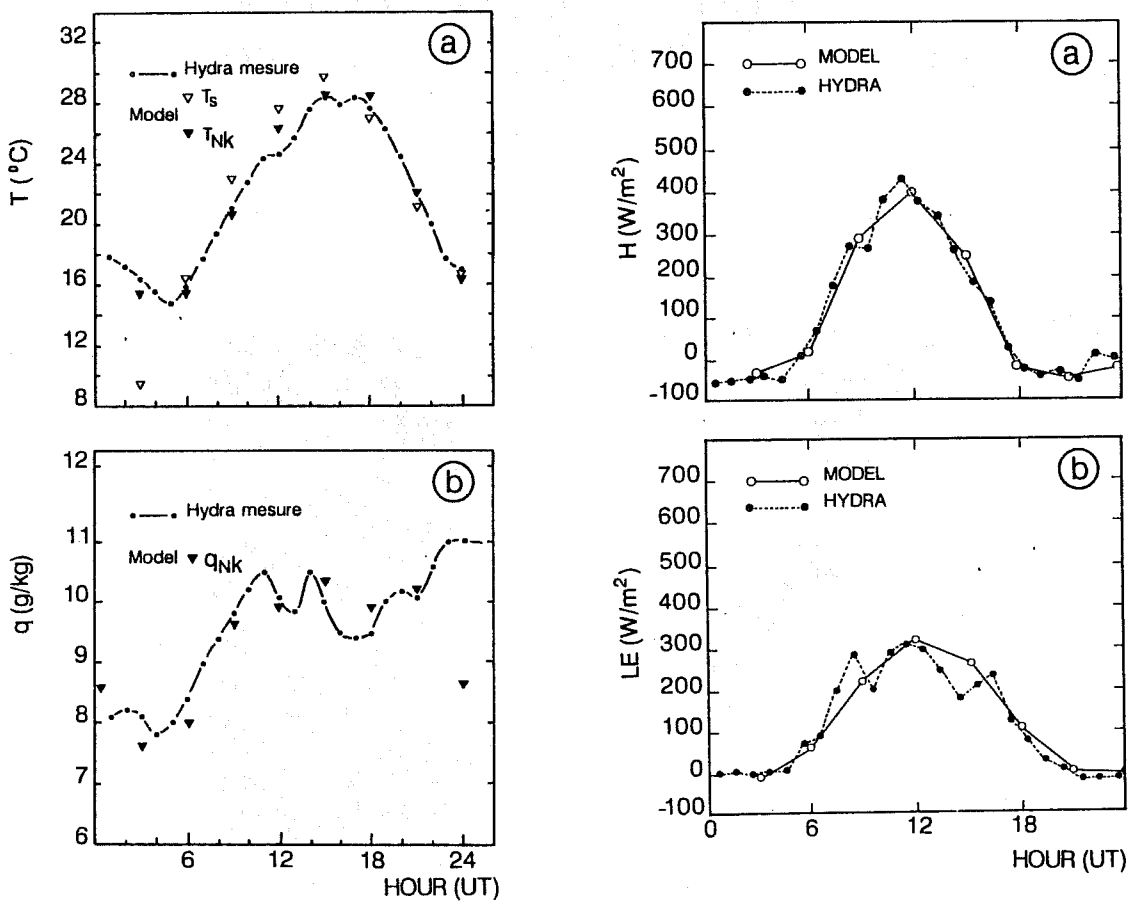

Fig. 13 : Comparison of predicted and measured temperature (a) and humidity (b) over the forest.

Fig. 14 : Comparison of predicted and measured sensible heat flux (a) and latent heat flux (b) over the forest.

evolution of specific humidity after 2100 Z. The model drops rapidly, while in the observations,q increases to 11 g/kg. This is probably more related to an underestimation of the moisture in the maritime air mass which is advected over the domain at that time, than to a wrong behaviour of the surface scheme. Indeed, the error in the forecast of the specific humidity is seen at various places in the model, always starting with the arrival of the maritime airmass. Rapid variations in the observed specific humidity during the afternoon are not reproduced by the model. The origin of these variations is not known to the authors.

The diurnal evolution of the fluxes of sensible and latent heat are compared to the observations over the forest in Fig. 14. The agreement can be considered as excellent, especially if we take into account the large changes of the Bowen ratio during the day. The maximum values observed and predicted are about 300 W/m^2 for the latent heat flux and 400 W/m^2 for the sensible heat flux. However, during the morning and evening hours, the latent heat flux is larger than the sensible heat flux. The success of the model in reproducing this behaviour is due to the F_3 factor in Eq. 15, which introduces the dependance of the surface resistance upon the atmosphere moisture deficit, as first proposed by Jarvis et al. (1976), and verified on the Hapex-Mobilhy data by Gash et al. (1988).

We next compare the model results for a grid point situated in the southeastern corner of the study area with a set of four Samer stations describing various conditions present in this area. These stations are Caumont (A), over a field of soja, and Tieste (B), Castelnau (C), Fusterouau (D) in fields of corn with little development. The fraction of vegetation for the reference grid box of the model has the quite low value of 0.48. This allows for a significant heat flux into the ground. The comparison of the sensible heat flux is next shown in Fig. 15a. The model predicted values fall well within the observed range for this quantity. The differences between the four stations come from several factors : the different development of the culture, slightly different atmospheric conditions, and different soil moisture contents. Here, it is rewarding to see that the model is able to predict a kind of average. The agreement is not so good for the latent heat flux, shown in Fig. 15b. Here, the model predicts a value higher than the average between the four stations,but close to the Caumont observations. We have found several possible origins for this discrepancy. Firstly, the model predicted global solar radiation is larger than the average observations. This could be due either to measurement errors, since the two different measuring systems are not in agreement (see e.g. Goutorbe and Marre, 1988), or to the underestimation of possible aerosol effects by the model. There are also differences between the albedo observed in the different sites, and the mean albedo determined by remote-sensing used in the model, (see above). Further work is needed to establish the most probable reason. Secondly, the model-predicted Bowen ratio is wrong, since the sensible heat flux is approximately correct and the latent heat flux is underestimated. This calls for an error on the mean grid-box value of veg. In fact, the procedure described above is not designed to provide grid-box average values of veg in agreement with the local observations. Here, we must remember that there is no reason why the model-predicted values should coïncide with the means of the four Samer stations !

Finally, we will compare the model results from a grid-point in the southwestern corner of the study area with a single Samer station (Vicq). This station is placed in a field of corn situated in a clearing inside

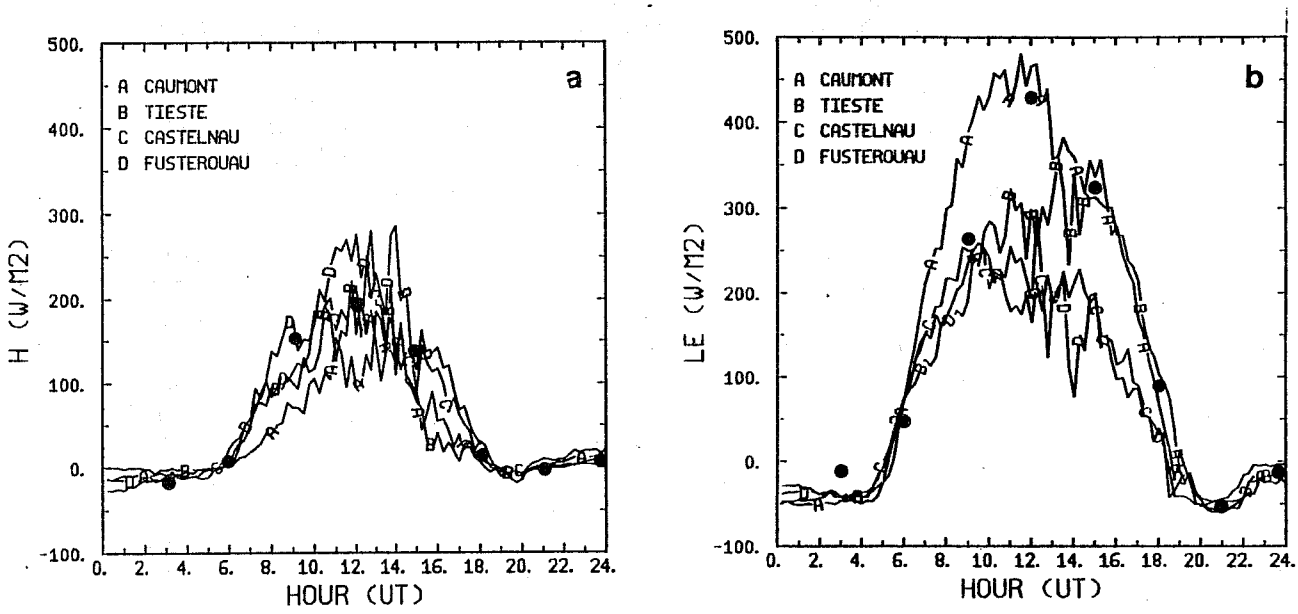

Fig. 15 : Comparison of sensible heat flux (a) and latent heat flux (b) observed and predicted by the model.

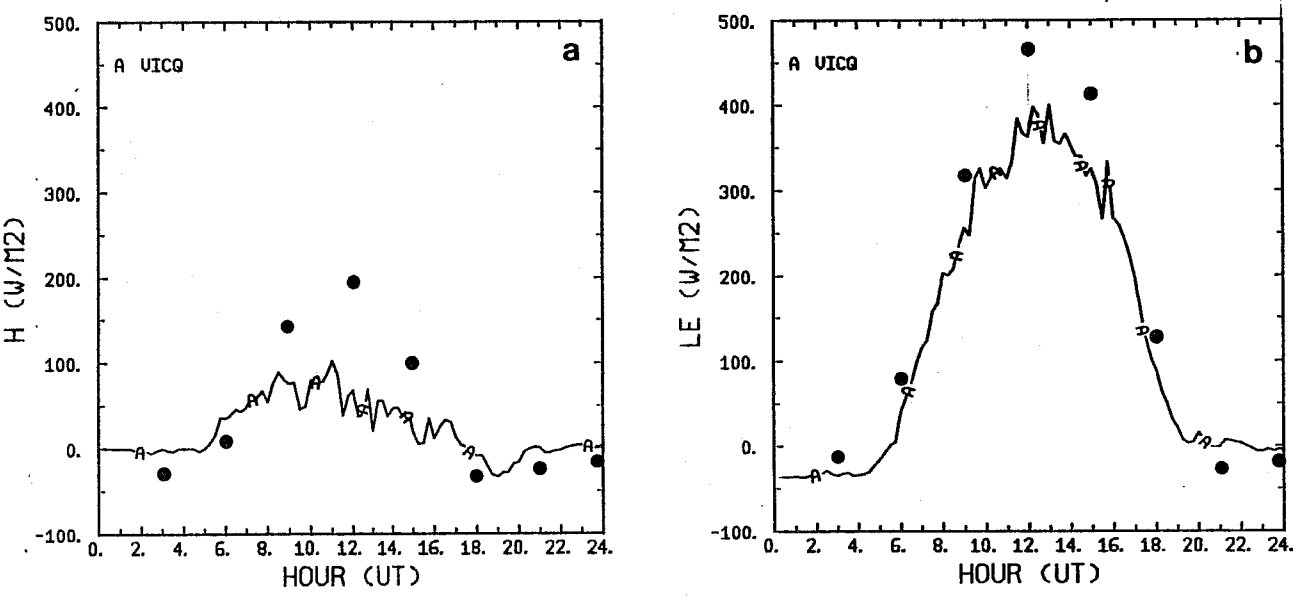

Fig. 16 : Sensible heat flux (a) and latent heat flux (b) observed at Vicq and predicted by the model.

the Landes forest. For a more significant comparison, we have chosen a model grid point with characteristics close to those of a crop area.

The net radiation is again overestimated by the model (see discussion above). As a consequence, the latent and sensible heat fluxes (Fig. 16) are overestimated but in very different proportions. The latent heat flux is overestimated by 10 %, and the sensible heat flux by more than 100 % ! The origin of this error on the Bowen ration can be ascribed to an oasis effect. Looking at the prediction of the wind speed, temperature and specific humidity at screen level, it is clear that the model understimates the temperature. We interpret this in relation with the fact that the station of Vicq is located in a clearing. The air temperature at Vicq is therefore very much influenced by the nearby forest, which is supposed to be warmer than the clearings. On the other hand, we have selected a "non-forest" grid point for comparison and the air temperature at this grid point is less influenced by the forest.
As a conclusion, these three comparisons between model-predicted quantities and local observations illustrate the complexity of this exercise. On the one hand, it is absolutely necessary to assess the general behaviour of the model, since local observations are at the present time the only sources which provide continuous information throughout the diurnal cycle of all quantities of interest. On the other hand, it should not be expected of the model to exactly reproduce the measurements of a local station, or even of a group of stations, which are not, except on very special cases, representative of the regional scale.

One never knows, whenever discrepancies are noted between model results and local observations, what part of these discrepancies should be attributed to model deficiencies, and what part to the non representativity of the measurements.

One way to escape to this problem is to use aircraft measurements. This has been the major axis of the Hapex-Mobilhy program strategy, and much is expected from the comparison between model results and aircraft flux measurements. Extensive comparisons have not yet been possible because the processing of aircraft data is still underway. We will, however, show a preliminary result which compares the June 16 simulation results, with the aircraft measurements contained in the draft report. The attention of the reader is drawn to the fact that those are preliminary and not yet validated results (Hildebrandt, 1987). To make this comparison, the aircraft trajectory (see Fig. 12) has been computed on the model horizontal and vertical grid. For each 20 km segment for which measurements are available, we have interpolated the model result at 1200 Z. The comparison is made with the "synthetic" 1200 Z aircraft measurement, which is obtained by combining of three actual measurements taken at different times, depending on the aircraft motion on its trajectory. These measurements are taken, at an altitude of 100 m above ground level. Comparison is shown in Fig. 17 for the turbulent kinetic energy, the sensible heat flux and the latent heat flux. It should be noted that the turbulent kinetic energy from the model is also interpolated at 100m above ground level (the model ground), but the sensible and latent heat fluxes are surface fluxes (we intend to use the fluxes computed at the altitude of 100 m for further work). There is clearly a satisfactory correspondance for both turbulent kinetic energy and sensible heat flux. The only visible regional contrast is between the forested and non-forested areas. The model reproduces the observed increase of sensible heat flux (from 150 W/m^2 to 300 W/m^2) and

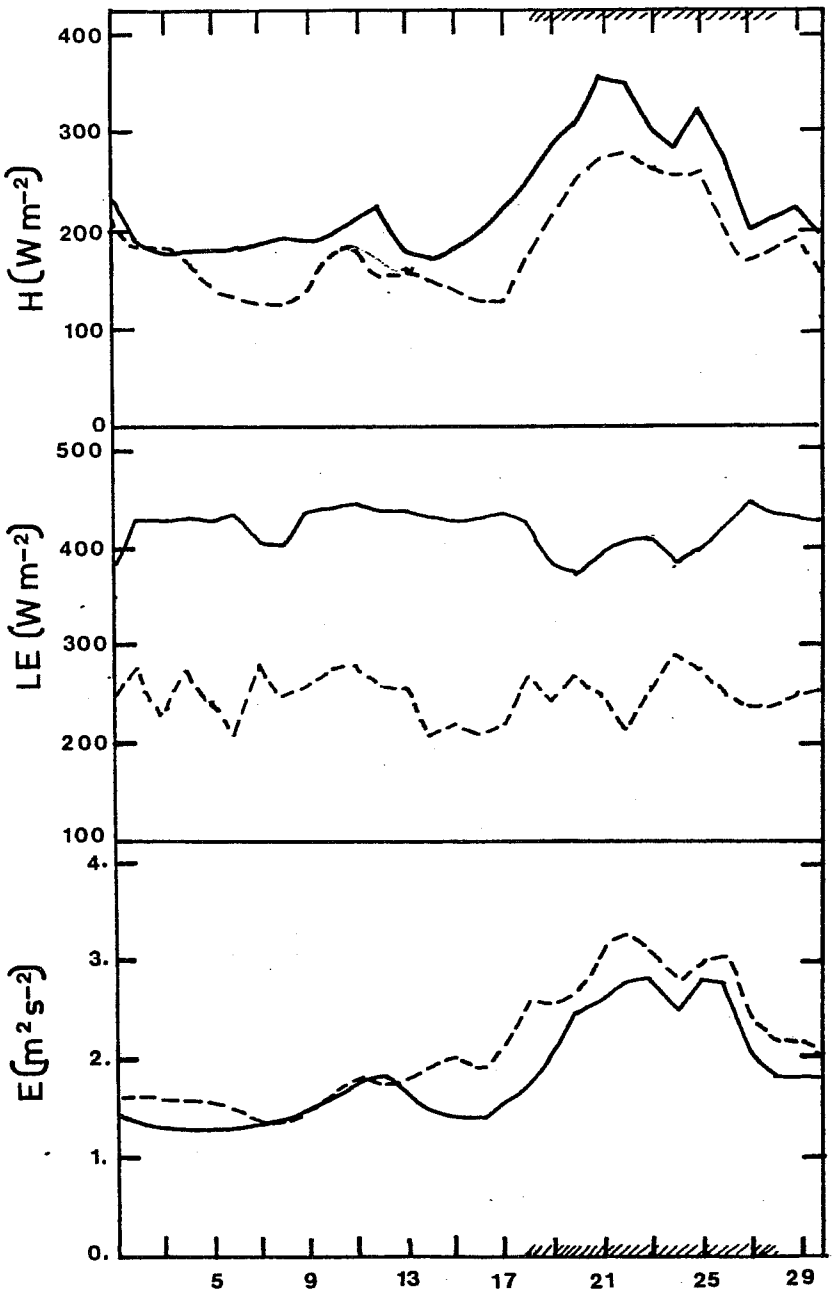

Fig. 17 : Sensible heat flux, latent heat flux and turbulence kinetic energy from aircraft measurements and model.

turbulent kinetic energy (from 1,5 m^2s^{-2} to 3 m^2s^{-2}) over the Landes forest. This result may be considered as one of the main success of the mesoscale modeling program for Hapex-Mobilhy, if the aircraft measurements are qualified in the near future.

Turning now to the comparison of the latent heat flux, it can be seen that the aircraft observations do not support the model results. The difference is as large as a factor of 2, the observations being smaller. This seems difficult to understand at the time this paper is written. One may of course question the empirical procedure that has been used to set the model parameters, and this will be done in the near future. However, it is puzzling to note that the disagreement is also present over the forest, where horizontal homogeneity is a good approximation. Moreover, one would expect a closer agreement between the Hydra station measurements (see Fig. 14 above) and the aircraft. Taking into account the fact that the aircraft fluxes are preliminary results, we will not further discuss this point.

7 - CONCLUSION

As it is obvious from the previous sections, the present paper is an attempt to discuss some results from a work which is still underway. We have built a new method of parameterization for land-surface properties, which is more simple than most previous methods, but incorporates the essential physics of the processes under study. We have shown by a series of one dimensional experiments that this scheme has the capacity to reproduce correctly the surface energy budget at the local scale.For inclusion inside the mesoscale model, the problem of subgrid scale variability has been treated in a deliberately simplified manner, as a first attempt to investigate the difficulty, and in order to remain consistent with the amount of existing information. The subgrid-scale variability of the soil texture and water content was ignored. The subgrid scale variability of the vegetation cover was treated by linearly averaging the fraction of vegetation deduced at the AVHRR pixel scale by a combination of a supervised classification method on two clear NDVI images and a table of correspondance deduced from the one dimensional experiments. This method allows for the derivation of a map of the fraction of vegetation which has been used in the mesoscale model, in lieu of the local value of this parameter, whereas the other parameters were specified at the value corresponding to the dominant vegetation type inside the grid-box. The results of the mesoscale model show a high degree of realism, as regards to the simulation of atmospheric parameters. The apparent surface temperatures predicted by the model are in agreement with infrared satellite pictures. As regards to the regional surface energy budget, and the prediction of the sensible and latent heat flux, the limitations of local measurements to assess the quality of the model results have been discussed, and some comparisons with already available aircraft measurements have been shown.

Those support the model results for the sensible heat flux and turbulence kinetic energy. On the other hand, the aircraft measurements of latent heat flux are not in agreement with the model results, and the screen level temperatures of the model seem to be underestimated by 2-3 K as compared to conventional measurements. This calls for further tuning of the parameters of the scheme.

Provided that this problem be solved and in view of the general results we feel that given the degree of quality of the mesoscale analysis and

the amount of information available to qualify the model results, there is no basis, at present time, to increase the complexity of the basic parameterization scheme. The method to account for subgrid scale variability may need some refinement. It is most usefull to try to obtain similar results on other days of the S.O.P., taking into account the evolution of those parameters that describe the vegetation properties and the soil water content. The present technique to obtain the grid-average value of veg cannot be extrapolated outside the SOP, and our intention is to work out a method to obtain this parameter directly from the NDVI images, using our continuously expanding set of reference values deduced from the 1D calibration experiments. This,however will be a difficult task, because the NDVI evolution with time is function not only of veg but also of such parameters as R_{smin} and LAI.

ACKNOWLEDGMENTS

We gratefully acknowledge the splendid work of all our colleagues who have been involved in the Hapex-Mobilhy field phase. In addition, the present work was only made possible through intensive collaboration with P. Mascart and J.P. Pinty (LAMP), who elaborated the map of soil texture and depth, T. Phulpin and J.P. Jullien, who produced the various maps of vegetation type, and R.M. Thépenier, who worked out the albedo maps. Comparison with the aerological and aircraft data were made easier by software developed by J.L. Champeaux and P. Peris.

REFERENCES

André, J.C., et al., 1988 : Evaporation over land-surfaces : first results from Hapex-Mobilhy Special Observing Period. Annales Geophysicae, 6, to appear.

Bret, B., et P. Bougeault, 1988 : Simulation de quatre journées Hapex-Mobilhy à l'aide du modèle Péridot. Note EERM n° 211, 90 pp.

Bougeault, P., 1987 : Les enseignements des premières études utilisant les données du réseau automatisé PATAC. La Météorologie, VII série, n°17.

Bougeault, P., 1988 : Parameterization schemes of land-surface processes for mesoscale atmospheric models. Proceedings of the Workshop on measurement and parameterization of land surface evaporation fluxes. 10-21 October 1988, Banyuls, France.

Bougeault, P., B. Bret, P. Lacarrère et J. Noilhan, 1988 : An example of spatial integration of a land surface parameterization in a meso-scale model. Proceedings of the Workshop on Measurement and Parameterization of land surface evaporation fluxes, 10-21 October 1988, Banyuls, France.

Clapp, R., and G. Hornberger, 1978 : Empirical equations for some soil hydraulic properties. Water. Resour. Res., 14, 601-604.

Cosby, B.J., G.M. Hornberger, R.B. Clapp, and T.R. Ginn, 1984 : A statistical exploration of the relâtionships of soil moisture characteristics to the physical properties of soils. Water Resour. Res., 20, 682-690.

Dedieu, G., P.Y. Deschamps, and Y.H. Kerr, 1987 : Satellite estimation of solar irradiance at the surface of the earth and of surface albedo using a physical model applied to Meteosat data. J. Clim. Appl. Meteor., 26, 79-87.

Durand, Y., et P. Bougeault, 1987 : L'analyse objective Péridot. Note EERM n° 193, 71 pp.

Gash, J.H.C., W.J. Shuttleworth, C.R. Lloyd, J.C. André, J.P. Goutorbe, and J. Gelpe, 1988 : Micrometeorological measurements in Les Landes forest during Hapex-Mobilhy. To appear in Agri. and Forest Meteorol.

Hildebrand, P., 1987 : Hapex flux and sounding data. Draft report.

Jarvis, P.G., 1976 : The interpretation of the variation in leaf water potential and stomatal conductance found in canopies in the field. Phis. Trans. Roy. Soc. London, B, 273, 593-610.

Goutorbe, J.P. and J.L., 1988 : Analyse du rayonnement - Période d'Observation Intensive. Expérience HAPEX-MOBILHY (available from CNRM).

Mascart, P., J. Gelpe, and J.P. Pinty, 1988 : Etude des caractéristiques texturales des sols dans la zone Hapex-Mobilhy 86. Note OPGC n° 95, 37 pp.

Mercusot, C., P. Bougeault, et Y. Durand, 1986 : Programme Hapex-Mobilhy. Atlas des analyses Péridot.

Monteith, J.L., 1976 : Vegetation and the atmosphere. Vol. 2 : Case studies. Academic Press, 439 pp.

Noilhan, J., and S. Planton, 1989 : A simple parameterization of land surface processes for meteorological models. To appear in Mon. Wea. Rev..

Phulpin, T., and J.P. Jullien, 1988 : A study of the vegetation cover with AVHRR during Hapex-Mobilhy. Proceedings of the 4th International Colloquium spectral signatures of objects in remote sensing. Aussois, France, 18-22 January, 1988.